Article

Numerical Modeling of Peridynamic Richards' Equation with Piecewise Smooth Initial Conditions Using Spectral Methods

Fabio V. Difonzo [1,*] **and Francesco Di Lena** [2]

1   Dipartimento di Matematica, Università degli Studi di Bari Aldo Moro, Via E. Orabona, 4, 70125 Bari, Italy
2   Istituto di Ricerca Sulle Acque, Consiglio Nazionale delle Ricerche, Via F. de Blasio 5, 70132 Bari, Italy;
    francesco.dilena@ba.irsa.cnr.it
*   Correspondence: fabio.difonzo@uniba.it

Abstract: In this paper, we introduce peridynamic theory and its application to Richards' equation with a piecewise smooth initial condition. Peridynamic theory is a non-local continuum theory that models the deformation and failure of materials. Richards' equation describes the unsaturated flow of water through porous media, and it plays an essential role in many applications, such as groundwater management, soil science, and environmental engineering. We develop a peridynamic formulation of Richards' equation that includes the effect of peridynamic forces and a piecewise smooth initial condition, further introducing a non-standard symmetric influence function to describe such peridynamic interactions, which turns out to provide beneficial effects from a numerical point of view. Moreover, we implement a numerical scheme based on Chebyshev polynomials and symmetric Gauss–Lobatto nodes, providing a powerful spectral method able to capture singularities and critical issues of Richards' equation with piecewise smooth initial conditions. We also present numerical simulations that illustrate the performance of the proposed approach. In particular, we perform a computational investigation into the spatial order of convergence, showing that, despite the discontinuity in the initial condition, the order of convergence is retained.

Keywords: Richards' equation; peridynamic theory; discontinuous initial condition; symmetric influence function

1. Introduction

Peridynamic theory is a relatively new mathematical framework, introduced by Silling in [1], that has gained attention in recent years for its ability to model fracture and damage in materials and to incorporate discontinuous solutions. Richards' equation is a classical partial differential equation that describes unsaturated water flow in porous media. In its standard formulation, porous media equations assume isotropic conditions (both in the saturated and unsaturated flow); indeed, experimental evidence has shown that several nonlocalities occur both in space and in time, as shown in [2,3] and as faced by computational tools in various situations (e.g., [4–6]).

An interesting issue related to Richards' equation consists of developing a general tool for dealing with the effects of dessication cracks in irrigation. Due to its nonlocal formulation, peridynamic theory appears to be a good framework to better investigate such problems related to Richards' equation.

Indeed, even if the introduction of nonlocalities increases the computational complexity, it allows, in several contexts, a more regular representation of the transient behavior of solutions at discontinuous interfaces, see, for instance, [7–10].

The numerical treatment of Richards' equation is still challenging because of its degenerate nature and the nonlinearity of its terms, and several numerical methods have been proposed recently (see, for instance, [11–19]).

In particular, recent results propose using spectral methods to discretize the model in space. For instance, in [20,21], the authors proposed a Fourier spectral method to

approximate the solution to both linear and nonlinear peridynamic equations, exploiting the convolutional form of the peridynamic model and the possibility to implement the FFT algorithm. In [22], an approach was introduced to efficiently compute weighted integrals using constrained mock Chebyshev least squares interpolation if the integrand function is known at a finite set of equally spaced nodes. However, such techniques either need to impose periodic conditions at the boundary or are not advisable in the case of an oscillating integrand function. A way to overcome this limitation consists of performing a volume penalization technique, which allows to enlarge the computational domain to a fictitious one to impose the periodic condition to such a new domain and then to penalize the solution to the reference domain, see [23,24], where such a method is proposed to study both a one-dimensional and a two-dimensional problem.

In [25–27], the authors proposed a different approach consisting of replacing the Fourier trigonometric polynomials by Chebyshev polynomials. The result is that, thanks to this approach, it is possible to recover the same accuracy obtained with the Fourier method, but periodic solutions are no longer required. Thus, this strategy does not require taking into account the computational cost of a volume penalization technique.

In this paper, we present a numerical model for solving the peridynamic Richards' equation with piecewise smooth initial conditions using the spectral method with Gauss–Lobatto nodes.

The spectral method is a powerful numerical technique that approximates a function using a truncated series of basis functions. Gauss–Lobatto nodes are a specific set of nodes that are used in the spectral method with Chebyshev polynomials as the basis functions. The use of Gauss–Lobatto nodes has been shown to improve the accuracy and efficiency of numerical simulations for a wide range of problems, including partial differential equations.

Following the idea of [25,28], in this paper, we use the spectral method with Gauss–Lobatto nodes to compute the numerical solution to the peridynamic Richards' equation with piecewise smooth initial conditions, and investigate the order of convergence of the method. Our numerical simulations demonstrate the effectiveness of the spectral method with Gauss–Lobatto nodes for solving the peridynamic Richards' equation and highlight its potential for future applications in related fields. In particular, our numerical results on spatial and temporal orders of convergence, which are retained in spite of the non-smoothness of the initial conditions, suggest that a suitable choice of the influence function, together with specific properties of spectral methods, sheds a light on a promising path for studies on transport problems in porous media which has not been investigated so far.

To the best of our knowledge, this is the first study to apply the spectral method with Gauss–Lobatto nodes to the peridynamic Richards' equation with piecewise smooth initial conditions. The results of this study contribute to the ongoing development of numerical methods for peridynamic theory and porous media simulations.

2. Mathematical Formulation

Richards' equation is a classical partial differential equation that describes the flow of water in porous media. In the peridynamic formulation of Richards' equation, the partial differential equation is replaced with an integro-differential equation that describes the flux of water at a point in the domain as a function of the displacement of the surrounding points. Specifically, the peridynamic Richards' equation can be written as:

$$\frac{\partial \theta}{\partial t} + \nabla \cdot \mathbf{q} = S \tag{1}$$

where θ is the water content, $\mathbf{q}$ is the Darcy flux, $S(\mathbf{x})$ is a source or sink term, and t is time. The Darcy flux, in our specific setting, is defined as:

$$\mathbf{q}(\mathbf{x}, t) = -\int_{\Omega} \frac{G(\mathbf{y} - \mathbf{x})}{\|\mathbf{y} - \mathbf{x}\|} \frac{K(\mathbf{x}) + K(\mathbf{y})}{2} [H(\mathbf{y}) - H(\mathbf{x})] \, d\mathbf{y} \tag{2}$$

where Ω is the domain of interest, K is the hydraulic conductivity, G is the peridynamic influence function, H is the water pressure, and $\mathbf{x}$ is the position vector.

The peridynamic influence function G is a nonlocal function that describes the interaction between two points in the domain. One common choice of peridynamic influence function is the Gaussian kernel:

$$G(r) = \frac{1}{(4\pi\delta^2)^{d/2}} e^{-r^2/(4\delta^2)}, \quad r \in [-1,1], \ \delta \in (0,1), \tag{3}$$

where d is the dimension of the domain and δ is the horizon, a parameter that determines the range of interaction between points. Note that, in general, peridynamic influence functions are required to be positive in $[-1,1]$ and symmetric with respect to the origin, and also their support must reduce as $\delta \to 0^+$.

However, as explained in Section 2.1 below, our choice will be different, mainly in order to avoid singularities arising in the numerical scheme proposed, where collocation points are not necessarily equally spaced.

Combining the above equations, we obtain the peridynamic formulation of Richards' equation:

$$\frac{\partial\theta}{\partial t}(\mathbf{x},t) + \nabla_{\mathbf{x}} \cdot \left(-\int_\Omega \frac{G(\mathbf{y}-\mathbf{x})}{\|\mathbf{y}-\mathbf{x}\|} \frac{K(\mathbf{x})+K(\mathbf{y})}{2} [H(\mathbf{y}) - H(\mathbf{x})] \, d\mathbf{y} \right) = S(\mathbf{x}) \tag{4}$$

with the initial condition:

$$\theta(\mathbf{x},0) = \theta_0(\mathbf{x}) \tag{5}$$

where $\theta_0(\mathbf{x})$ is the initial water content.

In summary, the peridynamic formulation of Richards' equation replaces the partial differential equation with an integro-differential equation that describes the flux of water at a point as a function of the displacement of the surrounding points. The use of peridynamic theory provides a powerful framework for modeling fracture and damage in porous media, and the peridynamic formulation of Richards' equation offers an alternative approach to modeling water flow in porous media that has advantages over classical partial differential equations.

2.1. Selection of the Influence Function

The selection of the influence function, as pointed out in (3), is a crucial issue in peridynamic modeling [29–31]. In a more general setting, $G(z) : \mathbb{R} \times \mathbb{R} \to \mathbb{R}$ represents a symmetric kernel, which can be defined as

$$G(z) = \chi_{B_\delta}(z) g(z), \tag{6}$$

where

$$\chi_A(z) = \begin{cases} 1, & z \in A, \\ 0, & z \notin A, \end{cases} \tag{7}$$

is the characteristic function relative to the domain A, $B_\delta := \{x \in \mathbb{R} : |x| < \delta\}$ for some $\delta > 0$, and $g(z)$ is the so-called scaled kernel and can have different forms. For example, it can be chosen as

$$g(z) := \frac{3}{\delta^3} \quad \text{or} \quad g(z) := \frac{2}{\delta^2} \frac{1}{|z|}. \tag{8}$$

Since our boundary conditions would typically be of Dirichlet type, we propose to consider an influence function concentrated on the horizon boundary of the form

$$G(x) := \begin{cases} \frac{|x|-1+\delta}{\delta}, & |x| \geq 1-\delta, \\ 0, & |x| < 1-\delta. \end{cases} \tag{9}$$

In so doing, the model is averaging the behavior around each point of the spatial domain. Thus, on the domain boundary, such a symmetric choice of influence function provides a nonlocal interaction with boundary conditions. Indeed, in this way, the local Dirichlet boundary conditions are influenced by the behavior of neighboring points, making them nonlocal, a condition that seems to be more appropriate in a peridynamic context, as shown in [32,33]. Moreover, using (9) turns out to be crucial for the boundedness of the peridynamic operator, which is necessary to prove convergence of the numerical scheme to the unique solution of (4). Moreover, such a model may suffer from instability at each $\mathbf{x} \in \Omega$ because of the singular integrand function in (4); our choice (9) would prevent any numerical bad behaviors. In fact, as witnessed in all our experiments, presented in Section 4, using (9) guarantees stability and convergence plus a reasonable shape of the numerical solutions.

3. Spectral Numerical Method with Gauss–Lobatto Nodes

To compute the numerical solution of the peridynamic formulation of Richards' equation, we used a spectral numerical method with Gauss–Lobatto nodes defined by

$$x_k = \cos\left(\frac{k\pi}{N}\right), \qquad k = 0, \ldots, N. \tag{10}$$

They are a set of points that are symmetrically spaced more closely near the boundaries of the domain and more widely spaced near the center. This distribution of nodes provides better accuracy near the boundaries, where the solution may vary rapidly. Moreover, this choice of nodes can limit and, in suitable cases, avoid the appearance of spurious oscillations (see [34]). In particular, as we will see in Section 4, even if we consider a discontinuous initial condition, the solution of the problem does not show any oscillations in its profile. The spectral method with Gauss–Lobatto nodes involves approximating the solution as a truncated series of Chebyshev polynomials:

$$\theta(x, t) \approx \sum_{n=0}^{N} \hat{\theta}_n(t) T_n(x) \tag{11}$$

where $T_n(x)$ is the n-th Chebyshev polynomial and $\hat{\theta}_n(t)$ are the coefficients of the series.

Substituting the above series into the peridynamic formulation of Richards' equation and projecting onto the Chebyshev basis functions, we obtain a system of ordinary differential equations for the coefficients:

$$\frac{d\hat{\theta}_n}{dt} = \sum_{m=0}^{N} M_{nm}(t) \hat{\theta}_m(t) + \hat{b}_n(t) \tag{12}$$

where $M_{nm}(t)$ is the time-dependent mass matrix and $\hat{b}_n(t)$ is the time-dependent source term [9].

The system of equations is solved using a time-stepping method, such as the backward differentiation formula (BDF) or the Runge–Kutta method.

More specifically, let us define the peridynamic operator as

$$\mathcal{L}(\theta) := \int_\Omega \frac{G(y-x)}{\|y-x\|} \frac{K(x) + K(y)}{2} [H(y) - H(x)] \, dy. \tag{13}$$

Moreover, let S_N be the space of Chebyshev polynomials of degree N,

$$S_N := \text{span}\{T_h(x) \mid 0 \le h \le N\} \subset L_w^2([-1, 1]), \tag{14}$$

and $P_N : L_w^2([-1, 1]) \to S_N$ be an orthogonal projection operator

$$P_N u(x) := \sum_{h=0}^{N} \hat{u}_h T_h(x) w_h, \quad u \in L^2_w([-1, 1]) \tag{15}$$

for w_h defined as

$$w_h := \begin{cases} \frac{\pi}{2N} & h = 0, N \\ \frac{\pi}{N} & h = 1, \ldots, N - 1, \end{cases} \tag{16}$$

and $w(x) = \left(\sqrt{1 - x^2}\right)^{-1}$.

We then propose to evaluate the Chebyshev transform of (4) to simplify the expression of the peridynamic operator on the right hand side, and then to integrate forward in time by using the explicit Euler scheme. Thus, our fully-discretized method reads

$$\theta^N_{m+1} = \theta^N_m + \Delta t \left(P_N \mathcal{L}(\theta^N_m) + P_N S(x) \right), \tag{17}$$

$$\theta^N_0(x) = P_N \theta^0_0(x), \tag{18}$$

where $\theta^N_m(x) \in S_N$ for every $m = 0, \ldots, N_T$.

4. Numerical Simulations

We present numerical simulations that illustrate the performance of the proposed approach. We consider a one-dimensional domain with a piecewise smooth initial condition. More practically, our method could be explained as follows:

1. We compute the Fourier transform of (4);
2. We generate Gauss–Lobatto collocation points in (10);
3. We integrate (17) and (18) by the forward Euler method;
4. We compute the inverse Fourier transform of the numerical solution to (17) and (18).

The numerical simulations show that the proposed peridynamic formulation can accurately model the flow of water through porous media, including situations where traditional formulations fail to capture the behavior.

We consider the classical van Genuchten–Mualem constitutive relations in the unsaturated zone given by

$$\theta(h) = \theta_r + \frac{\theta_S - \theta_r}{(1 + |\alpha h|^n)^m}, \quad m := 1 - \frac{1}{n},$$

$$K(h) = K_S \left[\frac{1}{1 + |\alpha h|^n} \right]^{\frac{m}{2}} \left[1 - \left(1 - \frac{1}{1 + |\alpha h|^n} \right)^m \right]^2,$$

where θ_r and θ_S represent the residual and the saturated water content, respectively, K_S is the saturated hydraulic conductivity, and α and n are fitting parameters.

The main aim of this paper is to numerically show how the spatial order of convergence, in contrast to typical examples in peridynamic theory, is preserved when imposing a piecewise smooth initial condition defined as:

$$\theta(x, 0) = \begin{cases} \theta_1(x), & \text{if } x < x_0, \\ \theta_2(x), & \text{if } x > x_0, \end{cases} \tag{19}$$

where $\theta_1(x)$ and $\theta_2(x)$ are suitable smooth functions and x_0 is the location of the discontinuity. The piecewise smooth initial condition is commonly used to model situations where the initial conditions change abruptly at a specific location. It is noteworthy that discontinuities have been faced in Richards' equation also considering piecewise continuous sink terms representing a root water uptake function, as in [35], or piecewise smooth hydraulic functions, as in [36,37]. However, it could be also possible that discontinuities in the initial condition may arise from ground data, so that they should be accurately located. Such issues that could be tackled by appropriate modeling of initial data dynamics can be treated

using numerical methods tailored for differential equations coming from semi-discretized version of advection–diffusion problems (see, e.g., [38,39]).

For the examples below, we report the convergence rates by varying the total number of collocation points used for spatial discretization and the time steps, validating our theoretical results. We fix the evaluation time and collocation point, and introduce the discrete relative L^2-error as follows

$$E_{L^2}^t = \frac{\sum_{h=0}^N \left| \theta^N(x_h, t) - \theta^*(x_h, t) \right|^2}{\sum_{h=0}^N \left| \theta^N(x_h, t) \right|^2}, \tag{20}$$

where $\theta^*(x, t)$ denotes the reference solution obtained by our method using a finer spatial mesh.

Example 1. *Drawing from [40], we consider a soil with the following parameters:*

$$\theta_r = 0.075, \ \theta_S = 0.287, \ \alpha = 0.036, \ n = 1.56, \ K_S = 0.94 \times 10^{-3} \, \text{cm/s}. \tag{21}$$

We add a sink term $S = -700 \, s^{-1}$ and parameter $\delta = 0.15$ in (9). We set our boundary conditions as follows

$$\theta(0, t) = 0.2234 \left(1 - \frac{t}{T} \right) + 0.181 \frac{t}{T}, \ t \in [0, T],$$

$$\theta(X, t) = 0.1368 \left(1 - \frac{t}{T} \right) + 0.1174 \frac{t}{T}, \ t \in [0, T],$$

while the initial condition is piecewise linear, defined as

$$\theta(\xi, 0) = \begin{cases} 0.2234 + (1 - \xi)(\bar{\theta} - 0.2234), & \xi \in [0, 1], \\ 2\bar{\theta} - \xi(0.1368 - 2\bar{\theta}), & \xi \in [-1, 0), \end{cases} \quad \bar{\theta} := \frac{0.2234 + 0.1368}{3}, \tag{22}$$

where $\xi := \frac{X - 2x}{X}, \ x \in [0, X]$. Here, $X = 30 \, cm$ and $T = 60 \, s$; moreover, we use $\Delta t = 0.06 \, s$ and $\Delta x = 0.3 \, cm$. The results are shown in Figure 1.
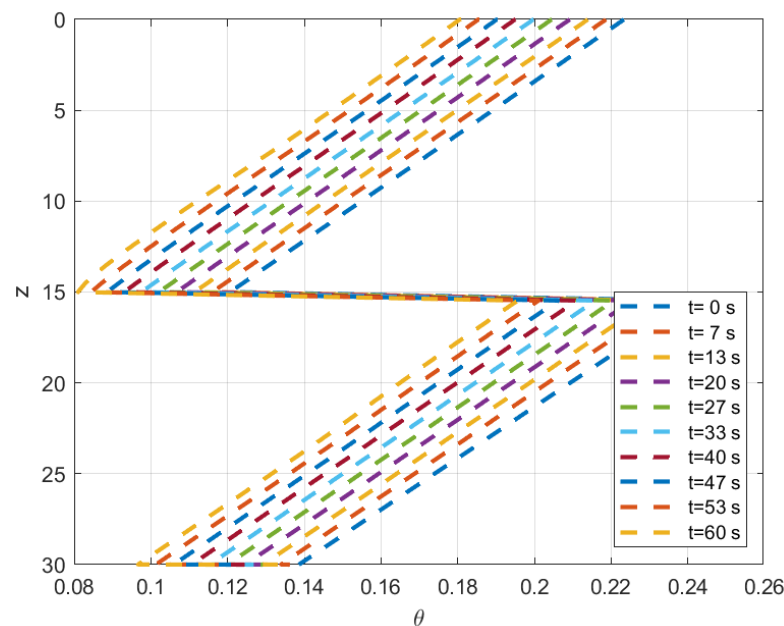

Figure 1. Numerical solution to Example 1.

In Table 1, we compute the discrete relative L²-error and the convergence rate with respect to the total number of meshpoints used to discretize in space and by fixing the time step.

Table 1. Numerical orders of convergence of the scheme with respect to the total number of collocation points relative to Example 1. The parameters for the simulation are $t = 60$ s and $\Delta t = 0.06$ s.

N	$E_{L^2}^t$	Convergence Rate
100	1.8451×10^{-4}	–
200	4.2273×10^{-5}	2.1259
400	9.1314×10^{-6}	2.1684
800	1.6716×10^{-6}	2.2579
1600	1.8546×10^{-7}	2.4577

Example 2. *In this example, the same soil as in Example 1 is considered, with the same parameters and the same boundary conditions; also, we add a sink term $S = -700\,s^{-1}$ and take $\delta = 0.15$ in (9).*
In contrast in the previous case, the initial condition is selected according to the formula

$$\theta(\xi, 0) = \begin{cases} 0.2234 - 0.0062(1 - \xi), & \xi \in [0, 1], \\ 0.1448 - 0.0062\xi, & \xi \in [-1, 0), \end{cases}' \tag{23}$$

where $\xi := \frac{X - 2x}{X}$, $x \in [0, X]$. Here, $X = 30$ cm and $T = 60$ s; moreover, we use $\Delta t = 0.06$ s and $\Delta x = 0.3$ cm. The results are shown in Figure 2. In Table 2, we compute the discrete relative L^2-error and the convergence rate with respect to the total number of meshpoints used to discretize in space and by fixing the time step. We can appreciate that, analogous to Example 1, the spatial order of converge is localized around 2 as the number of collocation points increases.
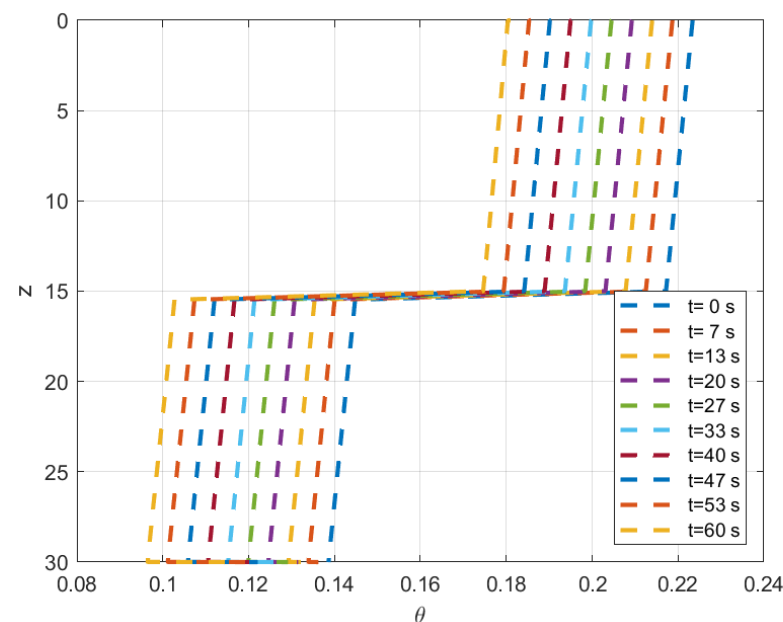

Figure 2. Numerical solution of Example 2.

Table 2. Numerical orders of convergence of the scheme with respect to the total number of collocation points relative to Example 2. The parameters for the simulation are $t = 60$ s and $\Delta t = 0.06$ s.

N	$E_{L^2}^t$	Convergence Rate
100	5.3499×10^{-7}	–
200	1.2318×10^{-7}	2.1188
400	2.6707×10^{-8}	2.1621
800	4.9001×10^{-9}	2.2517
1600	5.441×10^{-10}	2.4535

Example 3. *We consider a Berino loamy fine sand with the following parameters:*

$$\theta_r = 0.0286, \ \theta_S = 0.3658, \ \alpha = 0.0280, \ n = 2.2390, \ K_S = 0.006261 \,\text{cm}/\text{s}. \tag{24}$$

We have neither sink nor source, and we set parameter $\delta = 0.15$ in (9). *We set our boundary conditions as follows*

$$\theta(0, t) = 0.3, \ t \in [0, T],$$
$$\theta(Z, t) = 0.2, \ t \in [0, T],$$

while the initial condition is piecewise cubic, defined as

$$\theta(\xi, 0) = \begin{cases} 0.05\xi^3 + 0.25, & \xi \in [0, 1], \\ -0.05\left(\frac{\xi+5}{4}\right)^3 + 0.25, & \xi \in [-1, 0), \end{cases}' \tag{25}$$

where $\xi := \frac{X-2x}{X}$, $x \in [0, X]$. Here, $X = 30$ cm and $T = 6000$ s; moreover, we use $\Delta t = 6$ s and $\Delta x = 0.3$ cm. The results are shown in Figure 3.
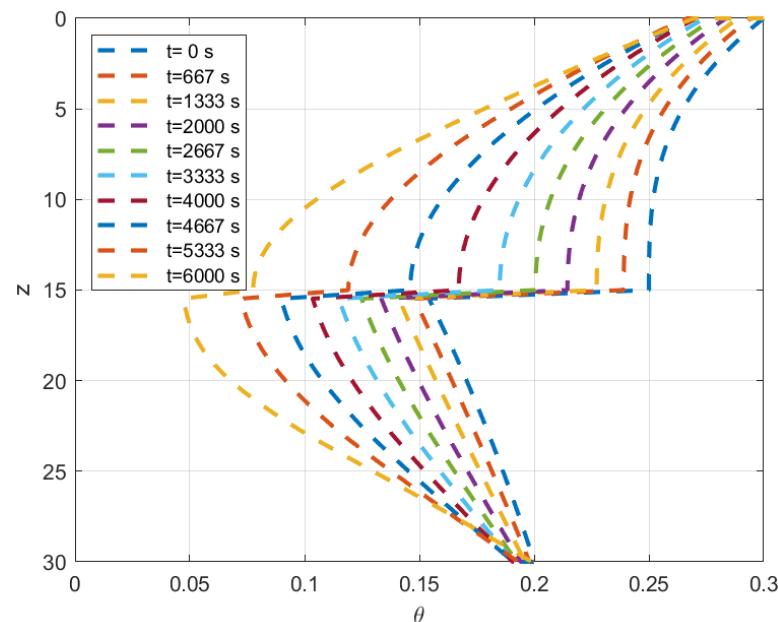

Figure 3. Numerical solution of Example 3.

In Table 3, we compute the discrete relative L^2-error and the convergence rate with respect to the total number of meshpoints used to discretize in space and by fixing the time step.

Table 3. Numerical orders of convergence of the scheme with respect to the total number of collocation points relative to Example 3. The parameters for the simulation are $t = 6000$ s and $\Delta t = 6$ s.

N	$E_{L^2}^t$	Convergence Rate
100	1.8215×10^{-3}	–
200	4.9081×10^{-4}	1.8919
400	1.1724×10^{-4}	1.9788
800	2.2719×10^{-5}	2.1041
1600	2.6015×10^{-6}	2.3336

Remark 1. *We witness that all our numerical experiments provide a temporal order of convergence equal to one. This is to be expected, since the spatial discontinuity in the initial condition does not affect the numerical integration forward in time.*

The results above suggest that a convergence result of the used spectral method should hold under hlconservative assumptions of the initial condition smoothness. In fact, since we used a second order discretization in space and the forward Euler method for integration in time, which is first order, we observed that such global orders of convergence are retained, in spite of discontinuities in the initial data. This behavior is interesting and unexpected, according to what usually happens using spectral methods [23,24].

5. Conclusions

In this paper, we have presented a numerical model for solving the peridynamic Richards' equation with piecewise smooth initial conditions using the spectral method with Gauss–Lobatto nodes. We have investigated the order of convergence of the method and compared it with other numerical methods commonly used for solving partial differential equations.

Our numerical simulations demonstrate that the spectral method with Gauss–Lobatto nodes is a powerful and efficient technique for solving the peridynamic Richards' equation with piecewise smooth initial conditions. We have shown that the spectral method with Gauss–Lobatto nodes has exponential convergence for smooth solutions, and that its accuracy can be improved by increasing the number of nodes used in the approximation. Furthermore, the use of Gauss–Lobatto nodes has advantages over other numerical methods, such as finite differences and finite elements, in terms of accuracy and efficiency.

The results of this study have important implications for the modeling and simulation of peridynamic theory and flow in porous media. The spectral method with Gauss–Lobatto nodes has the potential to provide accurate and efficient solutions to a wide range of problems in these fields, and its effectiveness for solving the peridynamic Richards' equation with piecewise smooth initial conditions highlights its versatility and potential for future applications.

In conclusion, the spectral method with Gauss–Lobatto nodes is a powerful and effective numerical technique for solving partial differential equations, and its application in peridynamic theory and porous media simulations is a promising area for future research.

Author Contributions: Conceptualization, F.V.D.; methodology, F.V.D.; software, F.V.D. and F.D.L.; validation, F.V.D. and F.D.L.; formal analysis, F.V.D.; investigation, F.V.D.; resources, F.V.D. and F.D.L.; data curation, F.D.L.; writing—original draft preparation, F.V.D.; writing—review and editing, F.V.D. and F.D.L.; visualization, F.V.D. and F.D.L.; supervision, F.V.D.; project administration, F.V.D. and F.D.L.; funding acquisition, F.V.D. and F.D.L. All authors have read and agreed to the published version of the manuscript.

Data Availability Statement: No new data were created or analyzed in this study. Data sharing is not applicable to this article.

Conflicts of Interest: The authors declare no conflict of interest.

References

1. Silling, S. Reformulation of elasticity theory for discontinuities and long-range forces. *J. Mech. Phys. Solids* **2000**, *48*, 175–209. [CrossRef]
2. Masciopinto, C.; Passarella, G. Mass-transfer impact on solute mobility in porous media: A new mobile-immobile model. *J. Contam. Hydrol.* **2018**, *215*, 21–28. [CrossRef]
3. Coppola, A.; Gerke, H.H.; Comegna, A.; Basile, A.; Comegna, V. Dual-permeability model for flow in shrinking soil with dominant horizontal deformation. *Water Resour. Res.* **2012**, *48*. [CrossRef]
4. Leij, F.J.; Toride, N.; Field, M.S.; Sciortino, A. Solute transport in dual-permeability porous media. *Water Resour. Res.* **2012**, *48*. [CrossRef]
5. Municchi, F.; Di Pasquale, N.; Dentz, M.; Icardi, M. Heterogeneous Multi-Rate mass transfer models in OpenFOAM®. *Comput. Phys. Commun.* **2021**, *261*, 107763. [CrossRef]
6. Ben-Noah, I.; Hidalgo, J.J.; Jimenez-Martinez, J.; Dentz, M. Solute Trapping and the Mechanisms of Non-Fickian Transport in Partially Saturated Porous Media. *Water Resour. Res.* **2023**, *59*, e2022WR033613. [CrossRef]
7. Coclite, G.M.; Paparella, F.; Pellegrino, S.F. On a salt fingers model. *Nonlinear Anal.* **2018**, *176*, 100–116. [CrossRef]
8. Dal Santo, E.; Donadello, C.; Pellegrino, S.; Rosini, M. Representation of capacity drop at a road merge via point constraints in a first order traffic model. *ESAIM: M2AN* **2019**, *53*, 1–34. [CrossRef]
9. Pellegrino, S.F. On the implementation of a finite volumes scheme with monotone transmission conditions for scalar conservation laws on a star-shaped network. *Appl. Numer. Math.* **2020**, *155*, 181–191. [CrossRef]
10. Pazienza, A.; Pellegrino, S.F.; Ferilli, S.; Esposito, F. Clustering underlying stock trends via non-negative matrix factorization. In Proceedings of the CEUR Workshop Proceedings—1st Workshop on MIning DAta for Financial ApplicationS, MIDAS 2016, Riva del Garda, Italy, 19 September 2016; Volume 1774, pp. 5–16.
11. Miller, C.T.; Abhishek, C.; Farthing, M.W. A spatially and temporally adaptive solution of Richards' equation. *Adv. Water Resour.* **2006**, *29*, 525–545. [CrossRef]
12. Casulli, V.; Zanolli, P. A Nested Newton–Type Algorithm for Finite Volume Methods Solving Richards' Equation in Mixed Form. *SIAM J. Sci. Comput.* **2010**, *32*, 2255–2273. [CrossRef]
13. Lai, W.; Ogden, F.L. A mass-conservative finite volume predictor—Corrector solution of the 1D Richards' equation. *J. Hydrol.* **2015**, *523*, 119–127. [CrossRef]
14. Berardi, M.; Difonzo, F.V.; Lopez, L. A mixed MoL-TMoL for the numerical solution of the 2D Richards' equation in layered soils. *Comput. Math. Appl.* **2020**, *79*, 1990–2001. [CrossRef]
15. Gąsiorowski, D.; Kolerski, T. Numerical Solution of the Two-Dimensional Richards Equation Using Alternate Splitting Methods for Dimensional Decomposition. *Water* **2020**, *12*, 1780. [CrossRef]
16. Berardi, M.; Difonzo, F.V. A quadrature-based scheme for numerical solutions to Kirchhoff transformed Richards' equation. *J. Comput. Dyn.* **2022**, *9*, 69–84. [CrossRef]
17. Hoang, T.; Pop, I. Iterative Methods with Nonconforming Time Grids for Nonlinear Flow Problems in Porous Media. *Acta Math. Vietnam.* **2022**. [CrossRef]
18. Islam, M.S.; Paniconi, C.; Putti, M. Numerical Tests of the Lookup Table Method in Solving Richards' Equation for Infiltration and Drainage in Heterogeneous Soils. *Hydrology* **2017**, *4*, 33. [CrossRef]
19. Meng, Z.; Chi, X.; Ma, L. A Hybrid Interpolating Meshless Method for 3D Advection–Diffusion Problems. *Mathematics* **2022**, *10*, 2244. [CrossRef]
20. Coclite, G.M.; Fanizzi, A.; Lopez, L.; Maddalena, F.; Pellegrino, S.F. Numerical methods for the nonlocal wave equation of the peridynamics. *Appl. Numer. Math.* **2020**, *155*, 119–139. [CrossRef]
21. Pellegrino, S.F. Simulations on the peridynamic equation in continuum mechanics. In *13th Chaotic Modeling and Simulation International Conference, CHAOS 2020*; Springer Proceedings in Complexity; Springer: Cham, Switzerland, 2021; pp. 635–649. [CrossRef]
22. Dell'Accio, F.; Di Tommaso, F.; Nudo, F. Constrained mock-Chebyshev least squares quadrature. *Appl. Math. Lett.* **2022**, *134*. [CrossRef]
23. Lopez, L.; Pellegrino, S.F. A spectral method with volume penalization for a nonlinear peridynamic model. *Int. J. Numer. Methods Eng.* **2021**, *122*, 707–725. [CrossRef]
24. Lopez, L.; Pellegrino, S.F. A space-time discretization of a nonlinear peridynamic model on a 2D lamina. *Comput. Math. Appl.* **2022**, *116*, 161–175. [CrossRef]
25. Lopez, L.; Pellegrino, S.F. A non-periodic Chebyshev spectral method avoiding penalization techniques for a class of nonlinear peridynamic models. *Int. J. Numer. Methods Eng.* **2022**, *123*, 4859–4876. [CrossRef]
26. Lopez, L.; Pellegrino, S.F. A fast-convolution based space–time Chebyshev spectral method for peridynamic models. *Adv. Contin. Discret. Model.* **2022**, *2022*, 70. [CrossRef]

27. Lopez, L.; Pellegrino, S.F. Computation of Eigenvalues for Nonlocal Models by Spectral Methods. *J. Peridynamics Nonlocal Model.* **2021**. [CrossRef]

28. Berardi, M.; Difonzo, F.V.; Pellegrino, S.F. A numerical method for a nonlocal form of richards' equation based on peridynamic theory. *arXiv* **2023**, arXiv:2301.11642.

29. D'Elia, M.; Li, X.; Seleson, P.; Tian, X.; Yu, Y. A Review of Local-to-Nonlocal Coupling Methods in Nonlocal Diffusion and Nonlocal Mechanics. *J. Peridynamics Nonlocal Model.* **2022**, *4*, 1–50. [CrossRef]

30. Jabakhanji, R.; Mohtar, R. A peridynamic model of flow in porous media. *Adv. Water Resour.* **2015**, *78*, 22–35. [CrossRef]

31. Jabakhanji, R. Peridynamic Modeling of Coupled Mechanical Deformations and Transient Flow in Unsaturated Soils. Ph.D. Thesis, Purdue University, West Lafayette, IN, USA, 2013. Available online: https://docs.lib.purdue.edu/open_access_dissertations/147 (accessed on 25 January 2022).

32. Aksoylu, B.; Kaya, A. Conditioning and error analysis of nonlocal operators with local boundary conditions. *J. Comput. Appl. Math.* **2018**, *335*, 1–19. [CrossRef]

33. Zhou, K.; Du, Q. Mathematical and numerical analysis of linear peridynamic models with nonlocal boundary conditions. *SIAM J. Numer. Anal.* **2010**, *48*, 1759–1780. [CrossRef]

34. Canuto, C.; Quarteroni, A. Approximation results for orthogonal polynomials in Sobolev spaces. *Math. Comp.* **1982**, *38*, 67–86. [CrossRef]

35. Berardi, M.; D'Abbicco, M.; Girardi, G.; Vurro, M. Optimizing water consumption in Richards' equation framework with step-wise root water uptake: A simplified model. *Transp. Porous Media* **2022**, *142*, 469–498. [CrossRef]

36. Mohanty, B.P.; Bowman, R.S.; Hendrickx, J.M.H.; van Genuchten, M.T. New piecewise-continuous hydraulic functions for modeling preferential flow in an intermittent-flood-irrigated field. *Water Resour. Res.* **1997**, *33*, 2049–2063. [CrossRef]

37. Berardi, M.; Difonzo, F.V. Strong solutions for Richards' equation with Cauchy conditions and constant pressure gradient. *Environ. Fluid Mech.* **2020**, *20*, 165–174. [CrossRef]

38. Berardi, M.; Lopez, L. On the continuous extension of Adams-Bashforth methods and the event location in discontinuous ODEs. *Appl. Math. Lett.* **2012**, *25*, 995–999. [CrossRef]

39. Berardi, M. Rosenbrock-type methods applied to discontinuous differential systems. *Math. Comput. Simul.* **2014**, *95*, 229–243. [CrossRef]

40. Berardi, M.; Difonzo, F.; Notarnicola, F.; Vurro, M. A transversal method of lines for the numerical modeling of vertical infiltration into the vadose zone. *Appl. Numer. Math.* **2019**, *135*, 264–275. [CrossRef]